INTERNATIONAL JOURNAL FOR NUMERICAL AND ANALYTICAL METHODS IN GEOMECHANICS, VOL. 20, 457–488 (1996)

BOUNDARY ELEMENT ANALYSIS OF LINEAR THERMOELASTIC CONSOLIDATION

DAVID W. SMITH

Department of Civil Engineering and Surveying, The University of Newcastle, Newcastle 2308, Australia

AND

JOHN R. BOOKER

Centre for Geotechnical Research, School of Civil and Mining Engineering, The University of Sydney, Sydney 2006, Australia

SUMMARY

This paper presents a direct boundary element method of numerical analysis, formulated in the Laplace transform domain, for a plane strain analysis of a linear thermo-poro-elastic material consolidating in the presence of a heat source. The equations governing the behaviour of the material are assumed to be a set of self-adjoint and fully coupled linear equations. A physical intepretation of the constants appearing in the linear theory relevant to engineering applications is presented. A boundary integral equation is developed from the governing equations in a straightforward way using the properties of Dirac delta functions, and an approximate boundary element method of numerical analysis is implemented using the Green's functions derived previously by the authors. The numerical analysis presented is motivated by the engineering design of a heat generating radioactive waste repository located deep underground. For this reason, there is a description of the application of the boundary integral equation method presented to the numerical solution of several problems of theoretical and practical interest in the area of radioactive waste disposal in clay-like soils.

KEY WORDS: Linear thermo-poro-elastic materials; boundary element method; Green's functions; Dirac delta functions

INTRODUCTION

The introduction to this paper is three parts. The first part broadly describes the motivation for the engineering problem analysed, the second part details some of the pertinent behaviours of a heat generating source in a geological repository and the choice of an appropriate mathematical model, while the third part provides an overview of some relevant aspects of the boundary element method employed in this paper for the mathematical analysis. A more detailed review of the particular boundary element method adopted here and the reasons for this choice are provided in a later section.

(a) *The long-term storage option for the management of radioactive waste*

Radioactive wastes are generated from all radioactive materials employed by industry. It is well known that these waste materials can present a serious biological hazard, in some cases for many thousands of years. Even when radioactive materials are used by industry in a way that presents negligible risk to humans, it is the question of what to do with the radioactive waste generated by industry that has emerged as one of primary concern. Indeed, regardless of whether or not this public concern is justified, it has prevented the nuclear energy industry from developing as first

CCC 0363–9061/96/070457–32

Received 10 June 1994
Revised 2 January 1995

envisaged. Nevertheless, many countries currently derive a substantial amount of their electricity from the nuclear power industry. For example, Canada and the United Kingdom derive approximately 20% of their electricity from nuclear energy, Germany and Japan approximately 30%, Korea and Sweden 50% and France and Belgium 70%.[1] For this reason, radioactive waste management is a current concern of the engineering profession. Indeed, many long term radioactive waste management strategies are being actively researched at the present time, and in some cases facilities are in an advanced stage of development.

There are essentially three alternatives for the ongoing management of radioactive materials following their usage by industry, namely, dispersion of the radioactive materials within the environment, reprocessing and reuse of the radioactive materials and finally, the long term storage of the radioactive materials until such time as they no longer present a biological hazard.[2]

While dispersion of radioactive waste to the environment in such a way that the natural background radiation levels are immeasurably changed appears attractive for several reasons, biological research has indicated that there does not appear to be a threshold below which radiation causes no damage to living organisms. In other words, dispersion of radioactive substances to the environment would probably result in increased rates of mutagenicity within living organisms, thereby effectively ruling out this alternative. The preprocessing and reuse of transmutation of the radioactive materials are attractive alternatives which are actively being researched. However, at the present time, not all radioactive materials lend themselves to reprocessing and reuse or transmutation, and even when the reprocessing and reuse or transmutation alternative is adopted, radioactive wastes are still produced.[1]

This leaves us with the final alternative, storage of the radioactive materials until they no longer present a biological hazard. An important property of radioactive materials is that their radioactivity decreases over time, and given sufficient time, will eventually pose a very small risk to the biological environment. This results in the fortuitous fact that the biological hazard presented by the radioactive waste decreases over time as the uncertainty of over its possible fate increases, unlike hazards presented by many other toxic materials.

It is well known that the average rate at which radioactive nuclei decay varies, some radioactive material decaying to a small fraction of their initial radioactivity in a matter of minutes (eg. Tecnetium-93; used for medical imaging purposes), while other materials remain hazardous for many thousands of years (eg. Plutonium-240, produced from the nuclear fuel cycle, has a half-life of approximately 24,000 years[3]). We note here that Strontium-90 and Cesium-137, two radioactive wastes produced in the nuclear fuel cycle that present a serious biological hazard and produce large quantities of heat during their decay, both have half-lives of approximately 30 yr. For this reason, the half life of the radioactive material adopted in the illustrative examples is taken to be 30 yr.

The variation in the rate of radioactive decay does present the opportunity for the radioactive wastes to be separated into its component materials and managed separately. Alternatively, the radioactive waste may be stored and handled in a stepwise procedure over time, the procedures adopted reflecting the different properties of the radioactive waste over time. For example, most radioactive waste management plans call for Cesium-137 and Strontium-90 to be stored underwater for a period of 30–50 yr until the rate of heat generation diminishes to a more manageable level. As will be made clear, unless this approach is adopted, excessive temperatures may be generated in a long term storage facility. However, the fact remains that these materials must be stored safely, and a central question becomes where to store long-lived radioactive materials so that risk to the biological environment is minimized?

One alternative is to store the waste above ground. This proposal has the advantage that the waste can be monitored and maintenance of the container undertaken as required. However,

maintenance necessarily involves a commitment to the on-going costs involved in this approach. In addition, because of the ready accessibility of the waste, there would be a need to guard against its accidental or purposeful dispersion. Indeed it is the very uncertainty of human affairs and the complete certainty of long term danger presented by radioactive materials that raises concerns about above ground storage as a long-term management solution. Nevertheless, above ground storage is the preferred alternative for the short-term management of long-lived radioactive wastes.

A long-term storage possibility is to bury the radioactive material below ground. The waste could be stored at a location within the earth that is stable over geologic periods of time and if so desired, the location could be made quite inaccessible, an example being storage in deep ocean sediments.[4] If this option was adopted, it would effectively remove the concern of accidental or deliberate dispersion to the biological environment. As already noted, most countries with a nuclear industry have research programmes investigating the suitability of underground nuclear waste repository sites. Indeed, many countries are expected to have operational facilities early in the next century.

Essentially, three types of host materials are being investigated as possible candidates for long-term storage, namely, unfractured granitic or shale rock, salt formations and clay soils.[2,5,6] Each of these materials could, given suitable conditions, theoretically prevent the dispersion of the radioactive waste to the biological environment for millions of years.[5, 7, 8] Of course, to realize this potential requires a detailed understanding of the physical and chemical behaviour of the host material in the presence of the radioactive waste.

While there are proposals to store the waste in an unsaturated geologic environment and thereby minimizing the potential for groundwater contamination, most deep underground waste repositories are below the water table and the soil or rock may be considered to be saturated. When contemplating the design of unsaturated repositories, careful consideration needs to be given to possible long-term climatic changes leading to saturated conditions at some time in the future. On the other hand, repositories that are currently saturated may not be in the future, thereby offering the possibility of increased rates of radioactive gas migration through unsaturated soils. In this paper, further consideration is restricted to host materials that are completely saturated by water over the design life of the repository. It is expected, therefore, that the analysis presented would have relevance to the deep ocean sediment disposal option, and to most land based disposal options involving the waste being emplaced at considerable depth below the groundsurface. We note that in this case, the mathematical assumption of the host material being of infinite extent may represent a good approximation to the actual field situation, and favour the adoption of the boundary element method for the mathematical analysis.

(*b*) *Disposal of a heat generating waste in a geologic repository*

From a contaminant transport viewpoint, it is desirable to choose to site the repository within a material that is very impermeable. The reason for this is that the advective component of the contaminant transport is then negligible. In this case, the primary means of contaminant transport is due to diffusive transport of the contaminants along their respective chemical gradients. It is well known that diffusive processes are slow, thereby ensuring that the time required for the contaminant to reach the biological environment will be significant. Elementary considerations of solutions to the diffusion equation based on Fick's law, show that the time required for diffusive transport increases in proportion to the square of the diffusion length, and this simple observation provides valuable guidance in repository design. For example, a well documented case of diffusive transport through clay has been reported by Rowe and Quigley.[9] In

this study it was found that chloride, a conservative ion, migrated approximately 1.4 m through Sarnia clay over a period of 16 yr. It could, therefore, be predicted that a 10 m thickness of the same clay soil could provide a barrier for approximately 800 yr, while a 100 m thickness of clay could provide a barrier for approximately 80,000 years. Research has shown that there is justification for extrapolating diffusive behaviour to very long periods of time in the manner just illustrated. For example, Desoulniers *et al.*[10] and Rowe and Sawicki[11] have shown diffusion parameters obtained from one week long laboratory tests provide excellent predictions of diffusion profiles occurring after ten to twelve thousand years.

With regard to contaminant migration through soils ad rock, we note that it is well established that the rate of diffusion of contaminants through natural soils is considerably reduced when the contaminant sorbs onto the soil particles.[12] When sorption of the contaminant onto the soil particles is taken into account, it is likely that many clay soils would provide effective barriers for at least many hundreds of thousands of years.[5,6] Of course, if the sorptive capacity of the soil is to be relied upon as part of the engineered barrier preventing the dispersion of radioactive materials to the biological environment, it is critical that the sorption parameters be measured under conditions similar to those expected in waste repository, that is, at elevated temperature in a multicomponent contaminant environment,[13] We note in passing that the boundary element method of analysis, not unlike the analysis presented here, may be adapted to the analysis of contaminant migration though the host material.

From the above discussion it is evident that geologic materials could theoretically provide an effective barrier to the release of radioactive materials to the biological environment for very long periods of time. Indeed, it appears that geologic materials are potentially the most effective barier to the movement of radioactive wastes.[5] However, while a low permeability host material minimizes advective transport and so is desirable from a contaminant transport viewpoint, complications are presented by the radioactive waste generating heat and the two phase nature of saturated soil and rock. This can give rise to at least three potentially serious problems in clay-like soils.

The first is that it has been established that the thermal conductivity of most clay soils decreases as their temperature increases. Thus the possibility arises that an unstable physical process may be established, at least initially, giving rise to temperatures that are much higher than expected on the basis of a linear heat flow analysis.[14] The elevated temperatures may in turn lead to changes in material properties of the soil, including changes to the permeability, plasticity and sorptivity of the contaminant by the clay, leading to unsatisfactory performance of the natural barrier.[4] However, the behaviour of such a complex physical system can only be satisfactorily assessed at this stage by means of careful experimental investigations. For this reason, the possible implications of temperature dependent thermal conductivity are not pursued further here.

A second potential complication relates to the instability arising from the temperature dependence of the pore fluid density. When a light fluid overlies a heavier fluid a gravitational instability arises, and a small perturbation can lead to convective motion of the pore fluid.[15] However, it has been shown[16] that for relatively impermeable clay soils, such as the clays considered for the disposal of radioactive waste materials, convective pore fluid movement is negligible and heat transfer takes place primarily via conduction. For this reason, convective fluid movement and consequent convective heat transfer are not considered further.

A third potentially serious problem arises from the two phase nature of a saturated soil and the unusual physical properties of water. It is well established that water has a much larger coefficient of thermal expansion than clay soil particles. The differential expansion of the two phases upon heating leads to an increase in pore water pressure. According to the well established principle of

effective stress, the increase in pore water pressure in turn leads to a decrease in effective stress. If the decrease in effective stress is sufficiently large, the clay soil may yield, or fluidize,[4] or the clay soil may fracture,[17] in each case seriously compromising the effectiveness of the clay barrier. Counteracting the increase in pore water pressure due to differential expansion of the soil composite is the dissipation of the excess pore water pressure as the water flows through the permeable soil. Clearly, the interaction between the rate of pore pressure generation and the rate of pore pressure dissipation is of critical importance in determining whether the effective stress state in the soil is around the emplaced heat source.

Given the foregoing considerations, it may be concluded that the permeability of the clay should be as small as possible so as to minimize both advective and diffusive transport through clay soil and consequently, the likelihood of contamination of the biological environment by radioactive contaminants. However, if the permeability is too low, the build up of excess pore water pressure in the heated clay soil could result in the effective stress in the clay soil being substantially reduced, leaving the soil fabric susceptible to damage. The engineer responsible for the design of the radioactive waste repository in a clay-like soil is therefore concerned with optimizing the permeability of the clay with respect to both contaminant transport and thermal consolidation behaviour. Specifically, the design engineer requires minimum permeability of the clay soil compatible with an adequate effective stress state in the soil. This paper is concerned with a mathematical model and method of analysis that may assist an engineering optimization to be made with regard to the permeability of the host material surrounding a radioactive repository. In an important sense, the 'philosophy' adopted for the repository design has an important bearing of the mathematical model that is deemed appropriate for the engineering analysis of this optimization problem. One approach to the selection and design of nuclear waste repositories is technical conservatism. Indeed this approach is usually recommended by most government authorities.[1,8] In this case, only modest temperature rises in the soil are planned, while the permeability is chosen to be large enough to ensure excess pore pressures and are dissipated at a rate that avoids the disruption of the soil fabric.

It is suggested that a linear theory may prove adequate for a repository design based on technical conservatism. For example, Hueckel and Peano[18] indicate that European guidelines require that temperature increments in the soil close to the heat source should not exceed 80°C while the temperature increases at the ground-surface temperatures are not permitted to be greater than 1°C. Given these modest temperature increments, it would be expected that any significant non-linear behaviour and/or plastic deformation of the soil would be confined to a relatively small volume of soil around the waste canister itself. Indeed, this observation has been made previously by Hollister *et al.*[8] In this case, a linear model may well provide a reasonable first approximation to the assessment of a proposed design. We also note Hueckel and Peano's[18] observation that the European guidelines for thermal response of the geologic material to the heat source impose constraints that significantly affect the design of underground radioactive waste repositories, and for this reason an accurate thermal analysis becomes important.

An alternative design approach would attempt to understand and control the much more complicated behaviour that occurs in the soils at higher temperatures. The potential advantage of this approach is that heat generating waste could be placed in the repository at a significantly greater density than that possible using the technical conservatism design approach, thereby minimizing the physical size of the radioactive waste repository. However, the soil behaviour under these conditions is beyond the scope of the model and the analysis presented in this paper. The interested reader is referred to papers by Hueckel and Peano,[18] Britto *et al.*,[19] Lewis *et al.*[20,21]

(c) *Linear thermoelastic consolidation*

A detailed study, involving both numerical and experimental programmes, investigating the behaviour of kaolin clay soil exposed to a heat source is currently being undertaken at Cambridge University. As part of this research, a detailed analytic study of linear thermo-elastic consolidation with uncoupled heat flow has been undertaken and published in a series of papers by Booker and Savvidou,[22–25] These publications, together with a solution published by McTigue,[26] are to the author's knowledge, the only known analytic solutions of the equations of uncoupled linear thermoelastic consolidation.

To further refine the thermoelastic consolidation analysis of clay soils, a boundary element method for analysing a set of fully coupled equations of linear thermoelastic consolidation is developed here. It is wellknown that the boundary integral method is particularly well suited to the solution of problems involving a large domain with a small bounding surface, such as these which often occur in geotechnical applications. In some instances when the bounding surface is large, such as occur when analysing the behaviour of a semi-infinite half-space, it may be possible to satisfy the adjoint boundary conditions on that surface of the domain, thereby eliminating that surface from the boundary integral.[27] Given these advantages, the boundary element method has proven popular for geotechnical applications.

The boundary element method presented here has been developed in a series of publications by Smith and Booker. In the first instance, a boundary element method for the analysis of transient uncoupled thermoelasticity was developed and implemented.[28,29] The method was later extended to the boundary element analysis of fully coupled thermoelasticity.[30] Therefore, having developed and tested the boundary element method for the solution of the governing differential equations mentioned above, this paper presents a logical extension of this research, namely, the development of the boundary integral equation and its numerical implementation for solving the equations of fully coupled linear thermoelastic consolidation.

In passing we note that the Green's function facilitating the approximation of the boundary integral equation for fully coupled thermoelasticity using a boundary element method was presented by Nowacki[31] and again by Sladek and Sladek.[32] In addition, as first detailed by Biot,[33] a clear mathematical analogy exists between the equations of fully coupled thermoelasticity and the equations of poroelasticity due to the similarity between Fourier's law of heat conduction and Darcy's law of fluid flow. Accepting this, the Green's functions developed for fully coupled thermoelasticity may, with simple substitutions, be interpreted as the Green's functions for Biot's theory of consolidation. Nevertheless, the Green's functions for an infinite medium governed by Biot's equations of consolidation have also been presented by Cleary,[34] and more recently by Cheng and Predeleanu.[35]

Cheng and Predeleanu[35,36] have developed and implemented a boundary element method based upon a numerical analysis in the Laplace transform domain, not unlike the approach adopted by Booker and Smith.[28–30,37] Smith confirmed the feasibility of the approach detailed by Cheng and Predeleanu (1988), and obtained very accurate solutions using the Laplace transform boundary element method implemented using piecewise constant linear boundary elements. Smith[38] found that when integrations over the boundary elements were evaluated analytically, boundary element solutions remained accurate to within a distance of one-twentieth of the length of the boundary element from the bounding surface.

The boundary integral equation for fully coupled thermoelastic consolidation presented in this paper is derived using the properties of the Dirac delta function in quite a straightforward way. The boundary element method implemented here is based upon a geometrical approximation of the bounding surface using linear boundary elements, while the field quantities over the bounding

surface are approximated by piecewise constant functions, the function being constant over each boundary element. The Green's functions for the equations of fully coupled thermoelastic consolidation that are required for the boundary element analysis in one, two and three spatial dimensions, and in the Laplace transform and real time domains, have been presented by Smith and Booker.[39] In this paper, the validity of the proposed solution method is established by comparison of boundary element solutions with a known analytic solution to the equations of fully coupled thermoelastic consolidation, while the application of the boundary element method is illustrated by the solution of some problems of theoretical and practical interest concerning the disposal of radioactive waste in saturated clay-like soils.

We finally note that there now exists a substantial and growing literature to account for non-isothermal consolidation behaviour of soil and rock.[20-22,26,40-45] The theories presented by these authors vary in the generality of the formulation, and some cases include non-linear behaviour. When non-linear soil behaviour is modelled, resort is usually made to finite element techniques for solution of the governing equations.[18-21] However, as previously discussed, provided the temperature change is not too large, it is expected that a linear model of soil behaviour will provide an adequate first approximation to the behaviour of a real soil. In the event that non-linear behaviour close to the heater is anticipated and deemed significant, the preferred numerical modelling strategy may involve the use of finite elements to model the near-field behaviour and boundary elements to model the far-field behaviour. In any case, the boundary integral equation presented in this paper is based upon a quite general fully coupled linear model of thermoelastic consolidation that incorporates all the features described in the linear models presented in the papers above. A particular physical interpretation of the model constants, based upon conceptually realistic tests on soils, can be found in Appendix I.

GOVERNING EQUATIONS OF THERMOELASTIC CONSOLIDATION

In the following, indicial notation is used for brevity. The usual conventions of indicial notation apply and it is assumed that the indices range over the index sets x, y and x, y, z as required.

As discussed in the introduction, there are many theories, based on a variety of approximations, developed to consider the thermal consolidation of a porous solid. However, all of the linear approximations can be regarded as particular instances of the following general equations.

The equations of equilibrium,

$$\sigma_{lm,m} + f_l = 0 \tag{1}$$

Hooke's law,

$$\sigma_{lm} = \lambda e_v \delta_{lm} + 2Ge_{lm} - \chi_0 p \delta_{lm} \tag{2}$$

the strain–displacement relations,

$$e_{lm} = \tfrac{1}{2}(u_{l,m} + u_{m,l}) \tag{3}$$

the void occupancy equation,

$$-\chi_1 e_v + \int_0^t \frac{k}{\gamma_w} \nabla^2 p \, dt - Jp + Y_0 \theta + \int_0^t l = 0, \tag{4}$$

(where it is assumed that the Darcy's law of fluid flow is valid), and the entropy balance equation,

$$-\beta_1 e_v + Y_1 p + \int_0^t \frac{K}{T_0} \nabla^2 \theta \, dt - Z\theta + \int_0^t n = 0, \tag{5}$$

(where it is assumed that Fourier's law of heat conduction is valid and that temperature variations are small compared to the ambient absolute temperature). The field quantities contained in equations (1)–(5) are, σ_{lm}, the components of the incremental total stress tensor, e_{lm}, the components of the incremental strain tensor of the soil skeleton, e_v, the incremental volumetric strain of the soil skeleton, p, the excess pore fluid pressure, and θ, the increment of temperature above the ambient temperature,

while the source terms appearing in equations (1), (4) and (5) are, f_l, the components of distributed body force, l, the rate of injected volume per unit volume of a distributed fluid source, and n the rate of entropy input per unit volume of a distributed entropy source. G, λ, J, β_0, β_1, χ_0, χ_1, Y_0, Y_1, Z, are material constants appearing in the linear theory of thermoelastic consolidation. We note here that G, λ may be interpreted as the familiar Lame constants for the thermo-poro-elastic material under drained isothermal conditions, while the material constants in Darcy's and Fourier's law have their usual interpretation, viz., k is the fluid permeability, γ_w is the unit weight of pore fluid, K the thermal conductivity, and T_0 is the ambient absolute temperature. Physical interpretations of the remaining constants of the linear theory of thermal consolidation are presented in Appendix I.

BOUNDARY CONDITIONS FOR THE EQUATIONS OF THERMOELASTIC CONSOLIDATION

Of course, a solution of the equations of linear thermoelastic consolidation must satisfy the governing equations thoughout the domain of interest together with appropriate boundary conditions. The boundary conditions include the following:

Mechanical boundary conditions:

$$\sigma_{ij} n_j = T_j \tag{6}$$

$$u_j = D_j \tag{7}$$

where T_j represents the specified total boundary traction in the jth direction, D_j represents the specified boundary displacement in the jth direction and n_j represent the direction cosines of the outward normal to the surface S;

Thermal boundary conditions:

$$Mh_n + N\theta = W \tag{8}$$

where M, N and W are functions of position on the surface, and h_n is the heat flux normal to the boundary. By suitable specialization of the functions, either temperature or heat flux may be specified over a position of the boundary, or a linear combination of the temperature and heat flux may represent a convection boundary condition; and finally,

Seepage boundary conditions:

$$Ov_n + Pp = Q \tag{9}$$

where O, P and Q are functions of position on the surface and v_n is the Darcy velocity of the fluid normal to the bounding surface.

A BOUNDARY INTEGRAL EQUATION FOR THERMOELASTIC CONSOLIDATION

Introduction

While in principle a boundary integral equation and boundary element method to solve second order parabolic differential equations in the real time domain appears attractive, previous work has shown that this approach presents significant numerical difficulties, and in fact has been asserted to be impractical.[46] The reason this approach is computationally inefficient is that the integral of the product of the Green's function and the field gradient over the surface must be integrated over the entire time history of the heat flow. This is particularly onerous when a solution is desired at longer time periods. In addition, the matrices required to evaluate the unknown boundary quantities are different for each time chosen, and no computational benefits accrue from finding solutions at intermediate times.

These difficulties have lead to many suggestions for improving the computational efficiency and accuracy of solutions to parabolic equations solved using the boundary element method. Most alternatives are centred around time stepping procedures.[47–52] Time-stepping methods have the important advantage that the matrices required to evaluate the unknown boundary quantities remain unchanged provided the size of the time step does not change. However, time-stepping procedures have the disadvantage of introducing the solution for the previous time step as an initial condition for the current time step. Most importantly, the evaluation of general initial conditions usually requires the evaluation of domain integrals. This fact clearly undermines the primary attraction of boundary element methods, that is, the absence of domain integrals. Here we note in passing that Henry and Banerjee[53] have asserted that time stepping methods for solving the equations of uncoupled thermoelasticity, as detailed for example by Sharp and Crouch,[50] are also impractical.

In order to avoid domain integrations involved in time stepping boundary element schemes, yet retain the computational efficiency of this approach, various attempts have been made to approximate the initial conditions of a particular problem by shape functions that may be reduced to boundary integrations by means of the divergence theorem.[53,54] However, while this approach may be of computational advantage for some problems, we note that the accuracy of the method depends upon the accuracy with which the interpolation function can represent the initial condition. Clearly, this becomes more difficult when the initial condition involves large spatial gradients of the field variable as frequently occurs in applications. In this case of large spatial gradients, Henry and Banerjee[53] suggest that the domain can be divided into subregions and the initial condition in each subregion better approximated by the shape functions, but once again, the simplicity and therefore the attraction of the boundary element method becomes obscured. Clearly, much of the research to date has indicated that the solution of parabolic differential equations using the boundary element method presents significant intrinsic numerical difficulties.

Due to the difficulties noted above, an alternative approach, based upon the Laplace transform method, is employed here. This approach is appealing, as the Laplace transform method and the boundary element methods are both suited to the analysis of linear differential equations. Specifically, a Laplace transformation can temporarily remove the time dependence from the governing equations, transforming the partial differential equation into an ordinary differential equation. The boundary element method is then employed to perform the numerical analysis in the Laplace transform domain. Once the solution has been found in the Laplace transform domain, it can be numerically inverted to find the solution in the real time domain using an inversion algorithm (eg. Reference 55).

This numerical approach was first adopted by Rizzo and Shippy[56] for the solution of the heat flow equation. A boundary integral equation for coupled and uncoupled thermoelasticity in the Laplace and real time domains has also been presented by Sladek and Sladek,[32,57] and this approach was implemented to solve the equations governing uncoupled and coupled thermoelasticity.[28–30,58] As noted earlier, similar developments have taken place for the boundary element analysis of Biot's equations of consolidation (e.g. References 35 and 59).

Boundary integral equations

Given the demonstrated accuracy and efficiency of the Laplace transform boundary element method described by Smith and Booker[28–30] and Cheng and Detournay,[59] and the difficulties experienced by alternative boundary element formulations, we choose to develop a boundary element formulation in the Laplace transform domain. We note here that while it is a simple matter to incorporate steady state pore pressure and temperature distributions into the boundary element analysis in the manner described by Rizzo and Shippy,[56] it may be reasonably assumed that the excess pore pressure and ambient temperature distribution are spatially uniform for the case of a heat source placed in a geologic material, and therefore in the subsequent discussion initial conditions are taken to be zero.

We note here that in the following, we denote the Laplace transform of a function (g) by a superior bar, viz,

$$\bar{g} = \int_0^\infty \mathrm{e}^{-st} g \, \mathrm{d}t$$

A boundary integral equation may be found most simply by means of an equation of virtual work, eg. Betti's reciprocal theorem incorporating the Duhamel–Neumann body force analogy.[31,60] In this way we directly find,

$$\int_S (\bar{T}_l \bar{u}_l^* - \bar{T}_l^* \bar{u}_l) \mathrm{d}S + \int_V (\beta_0 \bar{\theta} \bar{e}_v^* - \beta_0 \bar{\theta} \bar{e}_v) \mathrm{d}V + \int_V (\chi_0 \bar{p} \bar{e}_v^* - \chi_0 \bar{p}^* \bar{e}_v) \mathrm{d}V$$

$$- \int_V (\bar{f}_l^* \bar{u}_l - \bar{f}_l \bar{u}_l^*) \mathrm{d}V = 0. \tag{10}$$

Now assuming $\chi_0 = \chi_1$, $\beta_0 = \beta_1$, and $Y_0 = Y_1$, the equations governing linear thermoconsolidation become self-adjoint in the Laplace transform domain. Equations (4) and (5) may be introduced into equation (10), and choosing the test function to satisfy the equations of linear thermoelastic consolidation, the divergence theorem leads directly to,

$$- \int_S (\bar{T}_l^* \bar{u}_l - \bar{T}_l \bar{u}_l^*) \mathrm{d}S + \frac{1}{sT_0} \int_S (\bar{h}_n \bar{\theta}^* - \bar{h}_n \bar{\theta}) \mathrm{d}S + \frac{1}{s} \int_S (\bar{v}_n \bar{p}^* - \bar{v}_n^* \bar{p}) \mathrm{d}S$$

$$- \int_V (\bar{f}_l^* \bar{u}_l - \bar{f}_l \bar{u}_l^*) \mathrm{d}S + \frac{1}{s} \int_V (\overline{N\theta}^* - \bar{N}^* \bar{\theta}) \mathrm{d}V - \frac{1}{s} \int_V (\bar{L} \bar{p}^* - \bar{L}^* \bar{p}) \mathrm{d}V = 0 \tag{11}$$

where, $\bar{T}_l$ are components of the surface traction vector, h_n is the heat flux normal to surface, v_n the Darcy fluid velocity normal to surface, and the starred quantities denote field quantities due to a test function. The test function may be chosen to be a Green's function,[39] that is, the 'free

space' solution to the governing equations linear thermoelastic consolidation. For example, if the Green's function is chosen to be an impulse point entropy source of strength N^{θ^*}, viz,

$$\bar{N}^* = N^{\theta^*}\,\delta(\mathbf{r} - \mathbf{r}_0) \tag{12}$$

or a impulse point fluid source of strength L^{f^*}, viz,

$$\bar{L}^* = L^{f^*}\,\delta(\mathbf{r} - \mathbf{r}_0) \tag{13}$$

or a constant point force of magnitude $f_l^{i^*}$ in each of the co-ordinate directions, viz,

$$\bar{f}_l^* = \frac{f_l^{i^*}}{s}\,\delta(\mathbf{r} - \mathbf{r}_0) \tag{14}$$

where $\mathbf{r}$ denotes a position vector, then the temperature, excess pore fluid pressure and displacement in each of the co-ordinate directions at a point may be expressed as a boundary integral equation. The integral equation may be found by noting the following property of delta functions,[27,61]

$$\int_V f(\mathbf{r})\,\delta(\mathbf{r} - \mathbf{r}_0) = f(\mathbf{r}_0). \tag{15}$$

and then proceeding formally by substituting equations (12)–(14) in turn into equation (11), adopting source strengths to be of unit magnitude and setting distributed body, fluid and entropy source for the unstarred system to zero. Adopting this approach, we find the following boundary integral equations,

$$\frac{\varepsilon(\mathbf{r}_0)\bar{\theta}(\mathbf{r}_0)}{s} = \int_S (\bar{T}_l^{\theta^*}\bar{u}_l - \bar{T}_l\bar{u}_l^{\theta^*})\,\mathrm{d}S - \frac{1}{sT_0}\int_S (\bar{h}_n\bar{\theta}^{\theta^*} - \bar{h}_n^{\theta^*}\bar{\theta})\,\mathrm{d}S - \frac{1}{s}\int_S (\bar{v}_n\bar{p}^{\theta^*} - \bar{v}_n^{\theta^*}\bar{p})\,\mathrm{d}S \tag{16}$$

$$\frac{\varepsilon(\mathbf{r}_0)\bar{p}(\mathbf{r}_0)}{s} = \int_S (\bar{T}_l^{f^*}\bar{u}_l - \bar{T}_l\bar{u}_l^{f^*})\,\mathrm{d}S - \frac{1}{sT_0}\int_S (\bar{h}_n\bar{\theta}^{f^*} - \bar{h}_n^{f^*}\bar{\theta})\,\mathrm{d}S - \frac{1}{s}\int_S (\bar{v}_n\bar{p}^{f^*} - \bar{v}_n^{f^*}\bar{p})\,\mathrm{d}S \tag{17}$$

$$\frac{\varepsilon(\mathbf{r}_0)\bar{u}_i(\mathbf{r}_0)}{s} = \int_S (\bar{T}_l^{i^*}\bar{u}_l - \bar{T}_l\bar{u}_l^{i^*})\,\mathrm{d}S - \frac{1}{sT_0}\int_S (\bar{h}_n\bar{\theta}^{i^*} - \bar{h}_n^{i^*}\bar{\theta})\,\mathrm{d}S + \frac{1}{s}\int_S (\bar{v}_n\bar{p}^{i^*} - \bar{v}_n^{i^*}\bar{p})\,\mathrm{d}S \tag{18}$$

where $\varepsilon(\mathbf{r}_0)$ is equal to one when $\mathbf{r}_0$ lies inside the domain, one-half when $\mathbf{r}_0$ lies on a smooth boundary and zero when $\mathbf{r}_0$ lies outside the domain. For equations (16)–(18), the superscript θ^* denotes the entropy source Green's function, f^* denotes the fluid source Green's function ad i^* denotes the Green's function for the point force in the ith direction. The spatial derivatives of the field quantities at any point may be found by choosing the starred thermo-poro-elastic state to be due to the derivative of the Dirac delta function. Employing the properties of the derivative of a Dirac delta function we find,[27,61]

$$\frac{\varepsilon(\mathbf{r}_0)\bar{\theta}_j(\mathbf{r}_0)}{s} = -\int_S (\bar{T}_{l,j}^{\theta^*}\bar{u}_l - \bar{T}_l\bar{u}_{l,j}^{\theta^*})\,\mathrm{d}S - \frac{1}{sT_0}\int_S (\bar{h}_n\bar{\theta}_j^{\theta^*} - \bar{h}_{n,j}^{\theta^*}\bar{\theta})\,\mathrm{d}S - \frac{1}{s}\int_S (\bar{v}_n\bar{p}_j^{\theta^*} - \bar{v}_{n,j}^{\theta^*}\bar{p})\,\mathrm{d}S$$

$$\frac{\varepsilon(\mathbf{r}_0)\bar{p}_j(\mathbf{r}_0)}{s} = -\int_S (\bar{T}_{l,j}^{f^*}\bar{u}_l - \bar{T}_l\bar{u}_{jl}^{\theta^*})\,\mathrm{d}S + \frac{1}{sT_0}\int_S (\bar{h}_n\bar{\theta}_j^{f^*} - \bar{h}_{n,j}^{f^*}\bar{\theta})\,\mathrm{d}S + \frac{1}{s}\int_S (\bar{v}_n\bar{p}_j^{f^*} - \bar{v}_{n,j}^{f^*}\bar{p})\,\mathrm{d}S$$

$$\frac{\varepsilon(\mathbf{r}_0)\bar{u}_{i,j}(\mathbf{r}_0)}{s} = \int_S (\bar{T}_{l,j}^{i^*}\bar{u}_l - \bar{T}_l\bar{u}_{l,j}^{i^*})\,\mathrm{d}S - \frac{1}{sT_0}\int_S (\bar{h}_n\bar{\theta}_j^{i^*} - \bar{h}_{n,j}^{i^*}\bar{\theta})\,\mathrm{d}S - \frac{1}{s}\int_S (\bar{v}_n\bar{p}_j^{i^*} - \bar{v}_{n,j}^{i^*}\bar{p})\,\mathrm{d}S \tag{19}$$

Of course, the heat and fluid flux may be found by substituting the temperature gradient and excess pore pressure gradient into Fourier's law of heat conduction and Darcy's law of fluid flow, respectively, while the stress at a point may be found from the strain displacement relations and Hooke's law.

BOUNDARY ELEMENT ANALYSIS OF LINEAR THERMOELASTIC CONSOLIDATION

For our purposes it will be assumed that the boundary of a two dimensional body can be approximated by N straight line segments, denoted here as $S_1, S_2, \ldots, S_N$. It is also assumed that the continuous functions of temperature, excess pore pressure, their spatial gradients, displacement and traction over the surface of the body may be approximated by discontinuous piecewise constant functions which are constant over each boundary element. Although higher order approximations of both surface geometry and boundary functions may be employed in the numerical approximation of equations (16)–(19), the simple approximations outlined above are sufficiently accurate to establish the validity of the proposed integral equation and numerical procedure.[29] With these assumptions equations (16)–(18) may be approximated by,

$$\frac{\varepsilon(\mathbf{r}_0)\bar{\theta}(\mathbf{r}_0)}{s} = \sum_{n=1}^{N}\left[\bar{u}_l\int_S \bar{T}_l^{\theta^*}\,dS_n - \bar{T}_l\int_S \bar{u}_l^{\theta^*}\,dS_n - \frac{1}{sT_0}\left(\bar{h}_n\int_S \bar{\theta}^{\theta^*}\,dS_n - \bar{\theta}\int_S \bar{h}_n^{\theta^*}dS_n\right)\right.$$
$$\left. - \frac{1}{s}\left(\bar{v}_n\int_S \bar{p}^{\theta^*}\,dS_n - \bar{p}\int_S \bar{v}_n^{\theta^*}dS_n\right)\right] \tag{20}$$

$$\frac{\varepsilon(\mathbf{r}_0)\bar{p}(\mathbf{r}_0)}{s} = \sum_{n=1}^{N}\left[\bar{u}_l\int_S \bar{T}_l^{f^*}\,dS_n - \bar{T}_l\int_S \bar{u}_l^{f^*}\,dS_n - \frac{1}{sT_0}\left(\bar{h}_n\int_S \bar{\theta}^{f^*}\,dS_n - \bar{\theta}\int_S \bar{h}_n^{f^*}dS_n\right)\right.$$
$$\left. - \frac{1}{s}\left(\bar{v}_n\int_S \bar{p}^{f^*}\,dS_n - \bar{p}\int_S \bar{v}_n^{f^*}dS_n\right)\right] \tag{21}$$

$$\frac{\varepsilon(\mathbf{r}_0)\bar{u}(\mathbf{r}_0)}{s} = \sum_{n=1}^{N}\left[\bar{u}_l\int_S \bar{T}_l^{i^*}\,dS_n - \bar{T}_l\int_S \bar{u}_l^{i^*}\,dS_n - \frac{1}{sT_0}\left(\bar{h}_n\int_S \bar{\theta}^{i^*}\,dS_n - \bar{\theta}\int_S \bar{h}_n^{i^*}dS_n\right)\right.$$
$$\left. - \frac{1}{s}\left(\bar{v}_n\int_S \bar{p}^{i^*}\,dS_n - \bar{p}\int_S \bar{v}_n^{i^*}dS_n\right)\right] \tag{22}$$

where $\int dS_n$ denotes the integral over the nth boundary element. A well posed boundary value problem will prescribe either a temperature or its gradient (or a linear combination of these), an excess pore water pressure or its gradient (or a linear combination of these) and either a displacement or a traction at each element comprising the boundary of the domain. For this reason, equations (20)–(22) cannot be employed immediately to estimate temperatures, excess pore pressures and displacements at points within the domain.

To estimate field quantities at interior locations, the unknown boundary quantities must first be estimated. To do this, the point $\mathbf{r}_0$ is chosen to be at the midpoint of a boundary element, so only boundary quantities appear in equations (20)–(22). In this case, the integral over the element containing the point $\mathbf{r}_0$ is interpreted in the sense of a limit as he singularity point approaches the boundary, or as a Cauchy principal value. By choosing the point $\mathbf{r}_0$ to be at the midpoint of each of the N boundary elements in turn, in the case of two spatial dimensions, $4N$ simultaneous equations are obtained in $8N$ unknowns. N of the $4N$ simultaneous equations are obtained from

equation (20), N equations from equation (21) and $2N$ equations from equation (22). In matrix form the simultaneous equations may be represented as,

$$\overline{GV}_1 = \overline{HV}_2 \tag{23}$$

where

$$\bar{V}_1^{\mathrm{T}} = (\bar{h}_{n_1}, \bar{v}_{n_1}, \bar{T}_{1x}, \bar{T}_{1y}, \ldots, \bar{h}_{n_N}, \bar{v}_{n_N}, \bar{T}_{Nx}, \bar{T}_{Ny}), \quad \bar{V}_2^{\mathrm{T}} = (\bar{\theta}_1, \bar{p}_1, \bar{u}_{1x}, \bar{u}_{1y}, \ldots, \bar{\theta}_N, \bar{p}_N, \bar{u}_{Nx}, \bar{u}_{Ny}) \tag{24}$$

In words, the vectors $\bar{V}$ represent the Laplace transforms of the actual boundary quantities at the midpoints of the boundary elements. In equations (24), the first subscript indicates the boundary element and where applicable, the second subscript indicates the co-ordinate direction. We now consider the global matrices $\bar{G}$ and $\bar{H}$. These matrices are fully populated and composed of submatrices as indicated below,

$$\bar{G} = \begin{bmatrix} \bar{G}_{11} & \cdots & \bar{G}_{1N} \\ \vdots & \bar{G}_{ml} & \vdots \\ \bar{G}_{M1} & \cdots & \bar{G}_{MN} \end{bmatrix}, \qquad \bar{H} = \begin{bmatrix} \bar{H}_{11} & \cdots & \bar{H}_{1N} \\ \vdots & \bar{H}_{ml} & \vdots \\ \bar{H}_{M1} & \cdots & \bar{H}_{MN} \end{bmatrix} \tag{25}$$

The global matrices are square, so M equals N. Now turning to the structure of the submatrices for two spatial dimensions, $\bar{G}_{ml}$ and $\bar{H}_{ml}$ are composed of the following elements.

$$\bar{G}_{ml} = \begin{bmatrix} \dfrac{1}{sT_0}\displaystyle\int \bar{\theta}_n^{\theta^*}(r)\,\mathrm{d}S_n & \dfrac{1}{s}\displaystyle\int \bar{p}_n^{\theta^*}(r)\,\mathrm{d}S_n & \displaystyle\int \bar{u}_{xn}^{\theta^*}(r)\,\mathrm{d}S_n & \displaystyle\int \bar{u}_{yn}^{\theta^*}(r)\,\mathrm{d}S_n \\ \dfrac{1}{sT_0}\displaystyle\int \bar{\theta}_n^{f^*}(r)\,\mathrm{d}S_n & \dfrac{1}{s}\displaystyle\int \bar{p}_n^{f^*}(r)\,\mathrm{d}S_n & \displaystyle\int \bar{u}_{xn}^{f^*}(r)\,\mathrm{d}S_n & \displaystyle\int \bar{u}_{yn}^{f^*}(r)\,\mathrm{d}S_n \\ \dfrac{1}{sT_0}\displaystyle\int \bar{\theta}_n^{x^*}(r)\,\mathrm{d}S_n & \dfrac{1}{s}\displaystyle\int \bar{p}_n^{x^*}(r)\,\mathrm{d}S_n & \displaystyle\int \bar{u}_{xn}^{x^*}(r)\,\mathrm{d}S_n & \displaystyle\int \bar{u}_{yn}^{x^*}(r)\,\mathrm{d}S_n \\ \dfrac{1}{sT_0}\displaystyle\int \bar{\theta}_n^{y^*}(r)\,\mathrm{d}S_n & \dfrac{1}{s}\displaystyle\int \bar{p}_n^{y^*}(r)\,\mathrm{d}S_n & \displaystyle\int \bar{u}_{xn}^{y^*}(r)\,\mathrm{d}S_n & \displaystyle\int \bar{u}_{yn}^{y^*}(r)\,\mathrm{d}S_n \end{bmatrix} \tag{26}$$

$$\bar{H}_{ml} = \begin{bmatrix} \dfrac{1}{sT_0}\displaystyle\int \bar{h}_{n_n}^{\theta^*}(r)\,\mathrm{d}S_n & \dfrac{1}{s}\displaystyle\int \bar{v}_{n_n}^{\theta^*}(r)\,\mathrm{d}S_n & \displaystyle\int \bar{T}_{xn}^{\theta^*}(r)\,\mathrm{d}S_n & \displaystyle\int \bar{T}_{yn}^{\theta^*}(r)\,\mathrm{d}S_n \\ \dfrac{1}{sT_0}\displaystyle\int \bar{h}_{n_n}^{f^*}(r)\,\mathrm{d}S_n & \dfrac{1}{s}\displaystyle\int \bar{v}_{n_n}^{f^*}(r)\,\mathrm{d}S_n & \displaystyle\int \bar{T}_{xn}^{f^*}(r)\,\mathrm{d}S_n & \displaystyle\int \bar{T}_{yn}^{f^*}(r)\,\mathrm{d}S_n \\ \dfrac{1}{sT_0}\displaystyle\int \bar{h}_{n_n}^{x^*}(r)\,\mathrm{d}S_n & \dfrac{1}{s}\displaystyle\int \bar{v}_{n}^{x^*}(r)\,\mathrm{d}S_n & \displaystyle\int \bar{T}_{xn}^{x^*}(r)\,\mathrm{d}S_n & \displaystyle\int \bar{T}_{yn}^{x^*}(r)\,\mathrm{d}S_n \\ \dfrac{1}{sT_0}\displaystyle\int \bar{h}_{n_n}^{y^*}(r)\,\mathrm{d}S_n & \dfrac{1}{s}\displaystyle\int \bar{v}_{n}^{y^*}(r)\,\mathrm{d}S_n & \displaystyle\int \bar{T}_{xn}^{y^*}(r)\,\mathrm{d}S_n & \displaystyle\int \bar{T}_{yn}^{y^*}(r)\,\mathrm{d}S_n \end{bmatrix} \tag{27}$$

where,

$$r = |\mathbf{r}_n - \mathbf{r}_{m0}|, \tag{28}$$

and $\mathbf{r}_{m0}$ represents the position vector of the Dirac delta function located at the midpoint of the mth boundary element, and $\mathbf{r}_n$ is a position vector that ranges over the nth boundary element.

There are thought, four boundary conditions specified at the midpoint of each boundary element, so $4N$ boundary conditions may be used to reduce equation (23) to a set of $4N$ simultaneous equations in $4N$ unknowns. After the solution of these equations, all boundary quantities are known or estimated and so equations (20)–(22) may be used to estimate the transformed temperatures, excess pore pressures and displacements at chosen points within the domain.

Of course, the accurate evaluation of boundary integrals is required for the accurate estimation of boundary unknowns, and again for the accurate estimation of the field quantities within the domain. Due to the simplicity of the geometric approximation by straight line elements, it is possible to evaluate the most important components of the surface integrals analytically. The integrals of the integrated Kelvin solution over straight line elements are well known (for example, Reference 63). Integrals of modified Bessel functions (appearing in the Green's functions for two spatial dimensions[39]) may be accurately evaluated by integrating the logarithmic component of the modified Bessel function analytically, and the remaining portion using 4-point Gaussian quadrature. The integral of the modified Bessel function over the boundary element containing the singularity point may be accurately evaluated using a series expansion.[63]

VERIFICATION OF PROPOSED BOUNDARY ELEMENT ANALYSIS OF LINEAR THERMOELASTIC CONSOLIDATION

For the purposes of verifying the proposed solution technique and use of the Green's functions, we consider a solid cylinder of radius a under conditions of plane strain shown in Figure 1. For the verification problem presented here, it is assumed that a constant heat source of negligible diameter is located along the axis of the cylinder of material, and that this surface is permeable, traction free and maintained at the initial ambient temperature. Heat is switched on instantaneously at $t = 0$.

Three clay-like soils are examined, with $c/\varkappa$ ratios of 1/3, 1 and 3 and material properties as shown in Table 1. The parameters c and $\varkappa$ are here defined to be,

$$c = \frac{k}{\gamma_w} \frac{1}{(J + \chi_0^2/M)}, \qquad \varkappa = \frac{K}{T_0} \frac{1}{(Z + \beta_0^2/M)} \tag{29}$$

where $M = (\lambda + 2G)$.

A comparison of analytic and numerical solutions to the problem described is made to establish the validity of the of the boundary element formulation presented previously. The results of a boundary element analysis using 64 piecewise constant boundary elements are presented in Figures 2–6. The results shown in these figures have been normalized. The

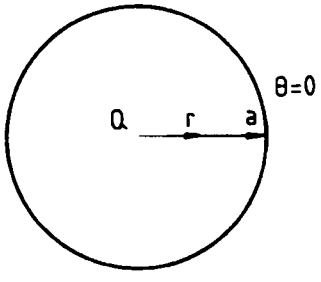

Figure 1. Thermal boundary conditions and geometry of solid cylinder

Table I. Material properties

Property	Value	Units
E	$2{\cdot}0 \times 10^{7}$	$\mathrm{N\,m^{-2}}$
v	$3{\cdot}0 \times 10^{-1}$	—
C_s	$1{\cdot}2 \times 10^{-11}$	$\mathrm{N^{-1}\,m^{2}}$
C_f	$4{\cdot}5 \times 10^{-10}$	$\mathrm{N^{-1}\,m^{2}}$
a_s	$1{\cdot}0 \times 10^{-5}$	$(^{\circ}\mathrm{C})^{-1}$
a_f	$6{\cdot}4 \times 10^{-5}$	$(^{\circ}\mathrm{C})^{-1}$
K	$2{\cdot}0 \times 10^{0}$	$\mathrm{W\,m^{-1}\,^{\circ}C^{-1}}$
T_0	$3{\cdot}5 \times 10^{2}$	K
n_0	$7{\cdot}0 \times 10^{-1}$	—
ϱ_s	$2{\cdot}4 \times 10^{3}$	$\mathrm{kg\,m^{-3}}$
ϱ_f	$1{\cdot}0 \times 10^{3}$	$\mathrm{kg\,m^{-3}}$
c_{ps}	$9{\cdot}5 \times 10^{2}$	$\mathrm{J\,kg^{-1}\,^{\circ}C^{-1}}$
c_{pf}	$4{\cdot}2 \times 10^{3}$	$\mathrm{J\,kg^{-1}\,^{\circ}C^{-1}}$

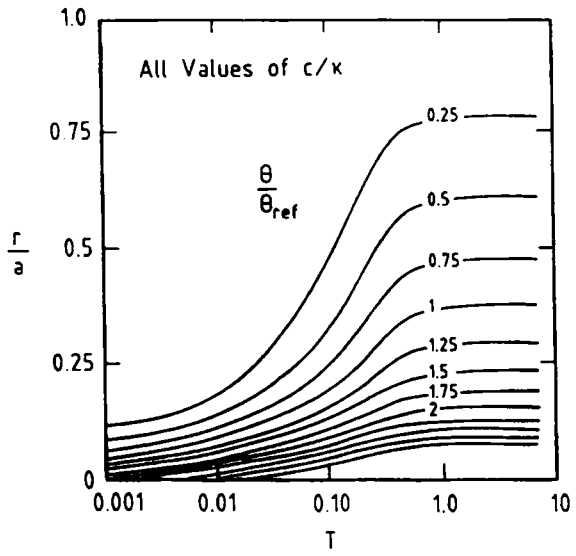

Figure 2. Isothermal contours of temperature in the spatial temporal domain for a cylinder of material with an axial heat source

temperatures are normalized by,

$$\theta_{\mathrm{ref}} = \frac{Q}{2\pi a K} \tag{30}$$

and the pore pressures by,

$$p_{\mathrm{ref}} = -\frac{c\gamma_f R_0 \theta_{\mathrm{ref}}}{k} \tag{31}$$

where,

$$R_0 = Y_0 - \chi_0 \beta_0 / M$$

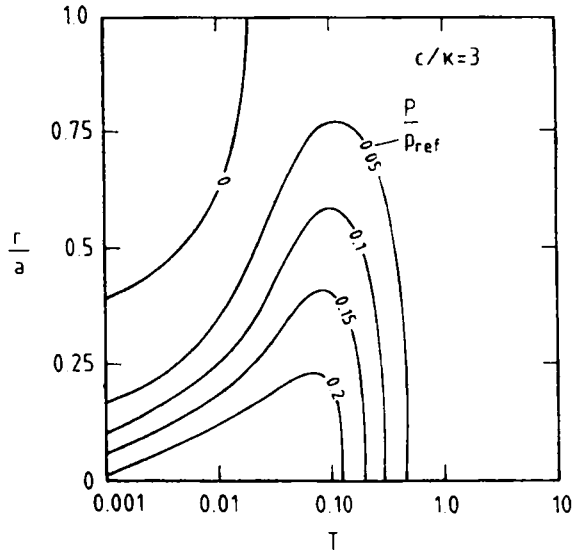

Figure 3. Isobaric contours of excess pore fluid pressure in the spatial temporal domain for a cylinder of material with an axial heat source; $c/\varkappa = 3$

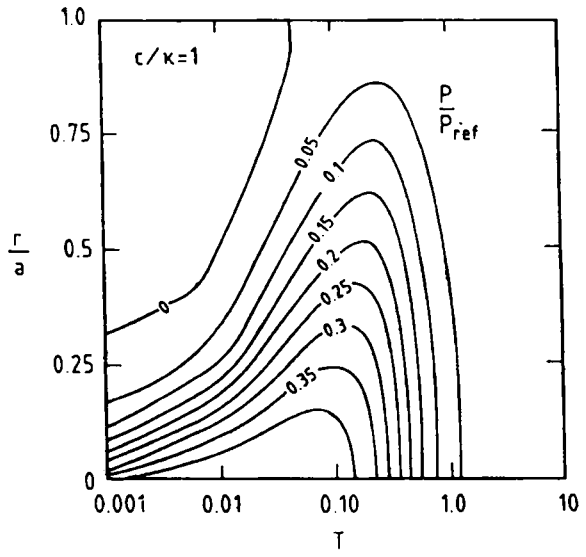

Figure 4. Isobaric contours of excess pore fluid pressure in the spatial temporal domain for a cylinder of material with an axial heat source; $c/\varkappa = 1$

Physically, p_{ref} may be interpreted as the final pore pressure generated at the surface of a cylinder of impermeable material subject to a temperature increase of θ_{ref}. The displacements are normalized by the final surface displacement of the cylinder, while the non-dimensional time is taken to be,

$$T = \frac{\varkappa t}{a^2} \tag{32}$$

where t is actual time.

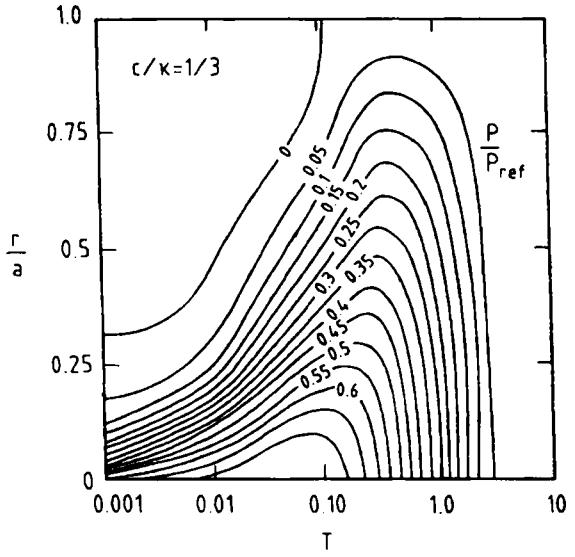

Figure 5. Isobaric contours of excess pore fluid pressure in the spatial temporal domain for a cylinder of material with an axial heat source; $c/\varkappa = 1/3$

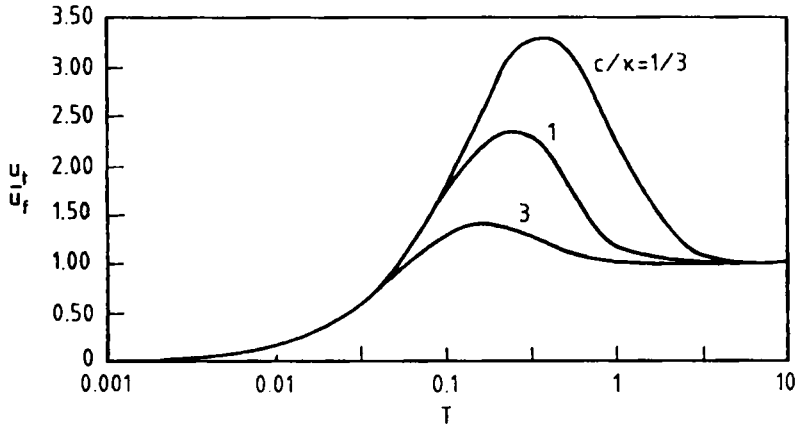

Figure 6. Evolution of the surface displacements over time of a cylinder of material for several $c/\varkappa$ ratios

The agreement between boundary element and analytic solutions was found to be excellent. As the solutions agree to within plotting accuracy, the two solutions are not differentiated in the Figures 2–6. Figure 2 shows the isothermal contours of the temperature distribution from time $t = 0$. As the temperature distribution over time is essentially unchanged by the $c/\varkappa$ ratio, it is concluded that the pore pressure coupling has an exceedingly small effect on the temperature distribution for the clay soil considered here. In addition, while the volume strain coupling effect on the temperature distribution increases with increasing thermal modulus, here it is shown to be exceedingly small for clay soils. We note in passing that even for thermal moduli appropriate for hard rock, the temperature distribution is usually changed by less than a few percent.[38] This

particular example serves to illustrate the more general conclusion that the temperature distribution within fine grained soils may be closely approximated using an uncoupled heat flow theory.[38]

Figures 3–5 show the variation of excess pore pressure in the spatial temporal domain for three $c/\varkappa$ ratios. It is observed that the results in each figure have a characteristic 'fingerprint' like pattern for each $c/\varkappa$ ratio. It is possible that by continuous monitoring of the excess pore fluid pressure and comparing experimental and theoretical 'fingerprints' of excess pressures in the spatial temporal domain, the estimation of this important material property may be facilitated.

Figure 6 shows the time variation of surface displacement. At earlier times, there is a gradual increase in the surface displacement reflecting both the thermal expansion of the pore water and soil skeleton. However, as the thermal expansion of the pore water is greater than that of the soil skeleton, the volume of the cylinder becomes larger than the cylinder's final volume in order to accommodate the expanded pore water at intermediate times. As the pore water moves to the surface, the soil consolidates to a volume determined by the thermal expansion of the soil skeleton alone.

We finally note that a companion verification analysis to the one detailed above has been presented in the paper by Smith and Booker.[39]

APPLICATIONS OF BOUNDARY ELEMENT METHOD TO THE ANALYSIS OF A RADIOACTIVE HEAT SOURCE BURIED DEEP IN A LINEAR THERMO-PORO-ELASTIC MATERIAL

In this section, we demonstrate some of the applications for which the numerical method previously detailed may be employed.

(*a*) *Base case*

For the purpose of illustration, the primary or base case considered here is that of a single long prismatic repository of square cross-section (two dimensional plane strain analysis), back-filled with a heat generating (radioactive) waste, embedded within an isotropic thermo-consolidating material of infinite extent. This primary option is compared and contrasted with alternative hypothetical waste disposal options. In all the options considered, initially the heat source is assumed to generate 1000 W m^{-1} run of repository, and that the heat source strength decreases exponentially over time a half life of 30 yr. Hence the heat flux normal to the tunnel wall is taken to be,

$$h_n = \frac{1000}{4a} e^{-0.023t} \tag{33}$$

where t is the time in years and a is the side length of the square, here taken to be 3·5 m. The wall of the square tunnel is assumed to be impermeable and fixed for the base case. All numerical results presented are obtained using 32 piecewise constant boundary elements to represent the boundary geometry of each surface, and material properties used are again as shown in Table I. The permeability of the clay for the analysis presented here is chosen to be $2{\cdot}25 \times 10^{-10}$ m s^{-1}, which is equivalent to a $c/\varkappa$ ratio of approximately 1·6. We note here that the assumed permeability is at least two orders of magnitude larger than the permeability of some clays being considered as a host material for a radioactive waste repository.[8,18] On the basis of the boundary element verification analysis already presented, we note that the excess pore water pressures

occurring in the clay soil will increase as the permeability decreases, and hence larger excess pore pressures would be expected in many cases of practical interest.

For the base case, the predicted temperature rise and excess pore pressure generated along the x-axis of a global co-ordinate system with origin at the centre of the square is shown in Figures 7 and 8. As expected, it is observed that the temperature and excess pore pressures are greatest

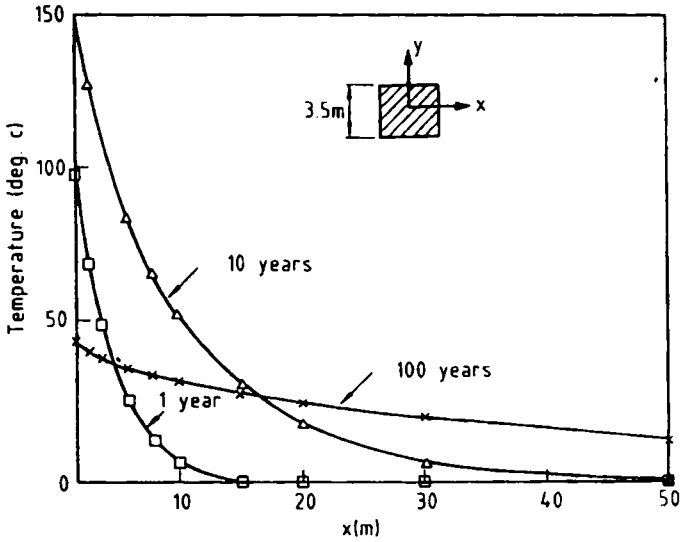

Figure 7. Temperature distribution at several times along the x-axis of a single square heat source

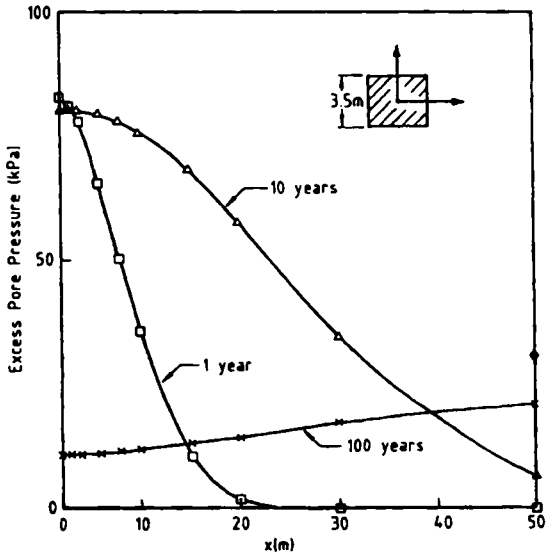

Figure 8. Excess pore pressure distribution at several times along the x-axis of a single square heat source

close to the square. The analysis reveals that the maximum value of the temperature is approximately 150°C and the excess pore pressure approximately 80 kPa, both occurring within the first 10 years after the placement of the heat source.

It is the observation that most of the heat is generated early in the life of the repository that gives rise to suggestions that the radioactive waste be stored temporarily for a number of years before being placed in an underground repository, thereby minimizing temperature and excess pore pressure changes.[4] As mentioned in the introduction, most radioactive waste management strategies called for above ground storage of the heat generating radioactive waste for the first 30–50 yr. After 30–50 yr, most of the high level radioactive waste would be generating heat at the rate of approximately 1.0–1.5 $kW\,m^{-3}$, which is approximately 12–18 times greater than the rate of heat generation adopted for this illustrative example. We note that even with this reduced rate of heat generation, the maximum temperature occurring in the clay soil is approximately 150°C, which clearly exceeds European repository design guidelines.[18]

Several alternative strategies may be adopted for reducing the maximum temperatures occurring in the clay adjacent to the heat generating waste. One alternative is to simply reduce the strength of the heat source, which is practical terms means a longer period of above-ground storage. As a linear mathematical model has been adopted here for the prediction of soil behaviour, proportionate scaling may be employed. For example, proportionate scaling predicts that a rate of initial heat generation equal to 500 $W\,m^{-1}$ run of tunnel would lead to a maximum temperature increase of approximately 75°C which is then within the European guidelines for repository design. Another alternative that will result in reduced soil temperatures is to increase the surface area to volume ratio of the repository while maintaining the same strength of the heat source, that is in practical terms, to place the heat generating waste in smaller repositories. Indeed, we note in passing that most radioactive waste disposal strategies adopt repository designs involving individual repositories of small cross-sectional area, thereby distributing the heat sources more evenly throughout the soil mass and so reducing maximum temperatures in the soil.

For the base case considered here, it is clear that the excess pore fluid pressures generated as a result of the heat source are unlikely to result in any significant disruption of the soil fabric when the repository is located at large depths below the ground surface. However, we note that if the repository is fairly close to the soil surface, as may occur with the deep ocean sediment disposal option, excess pore pressures generated have a much greater potential for compromising the soil barrier to the dispersion of radionuclides, especially if the clay has a very low permeability.

It is apparent from Figure 8 that at early times the excess pore pressure gradient tends to induce pore fluid flow away from the heat source. Indeed, the excess pressure gradients illustrated in Figure 8, together with Darcy's law of fluid flow, provide an opportunity to check the assumption that heat transport due to convection is negligible compared to conduction.[16] For example, after one year, the average excess pore pressure gradient is approximately 4·5 $kPa\,m^{-1}$, and given a permeability of $2{\cdot}25 \times 10^{-10}\,m\,s^{-1}$, the Darcy velocity is easily shown to be approximately 0·03 $m\,a^{-1}$. Therefore, as a first approximation, it is estimated that convective heat transport would lead to about 0.03 m displacement of the heat front, while Figure 7 shows that after one year diffusive heat transport has led to a significant increase in temperature greater than 10 m from the wall of the repository. It is therefore demonstrated that in this case the error induced by neglecting convective heat transport is negligible.

It is also interesting to note that at large times, the excess pore pressure gradient reverses, and therefore advective flow reverses (Figure 8). This would tend to further minimize the negligible error associated with neglecting convective heat transfer. It is noted in passing that the gradient reversal is linked to the relative rates of cooling of the heated pore fluid in the spatial domain, in

the same way that the excess pore pressure gradients are initially linked to the relative rates of heating of pore fluid.

Figures 9 and 10 show contours of the temperature and pore pressure changes around the square one year after emplacement of the heat source. It is seen that the geometrical effect of a square opening on the temperature and excess pore pressure fields is quickly lost, the contours becoming nearly circular a short distance from the wall of the opening. This is also true for the incremental total principal stress change contours shown in Figure 11, the contours becoming nearly circular within two side-lengths from the repository wall.

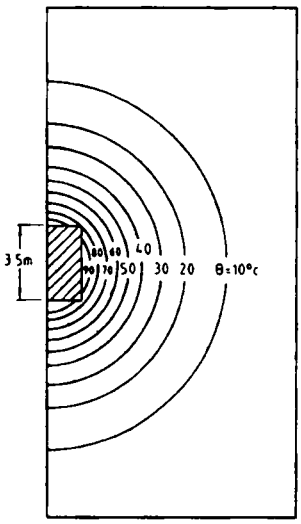

Figure 9. Contours of temperature surrounding a square exponentially decaying heat source 1 yr after placement of the source

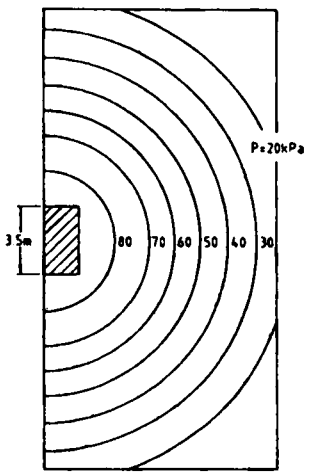

Figure 10. Contours of excess pore pressure surrounding a square exponentially decaying heat source 1 yr after placement of the source

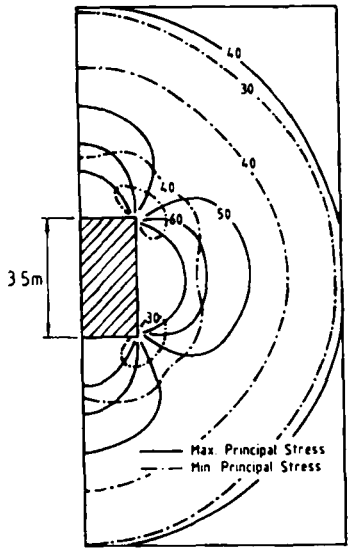

Figure 11. Contours of incremental maximum and minimum principal effective stress (kPa) surrounding a square exponentially decaying heat source 1 yr after placement of the source

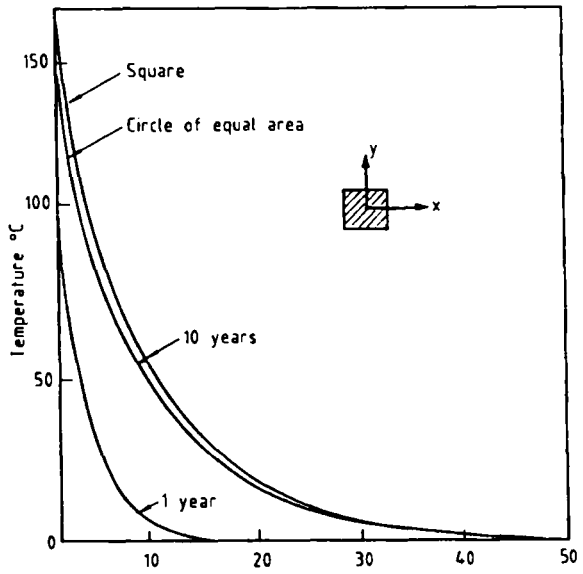

Figure 12. Comparison of the temperature distribution along the x-axis of a square heat source and a circular heat source of the same strength; square and circle are of equal cross-sectional area

(*b*) *Comparison of numerical solutions for square and circular openings*

The observation that temperature and excess pore pressure contours are nearly circular a short distance from the wall of the square prompts a comparison between solutions for the temperature increments along the x-axis in the base case with the temperature increments along a radii extending from a circular opening in an infinite solid. Figure 12 shows that the temperature

distribution at various times differs slightly when the circle has the same area as the square, while Figure 13 shows that the two solutions are nearly indistinguishable when the circle and the square have the same cross-sectional perimeter length.

These observations are confirmed by the contours of temperature, excess pore pressure and incremental total principal stress around a cylindrical heat source one year after emplacement shown in Figures 14 to 16. Outside, a circle of approximately 2.5 radii, the temperature, excess

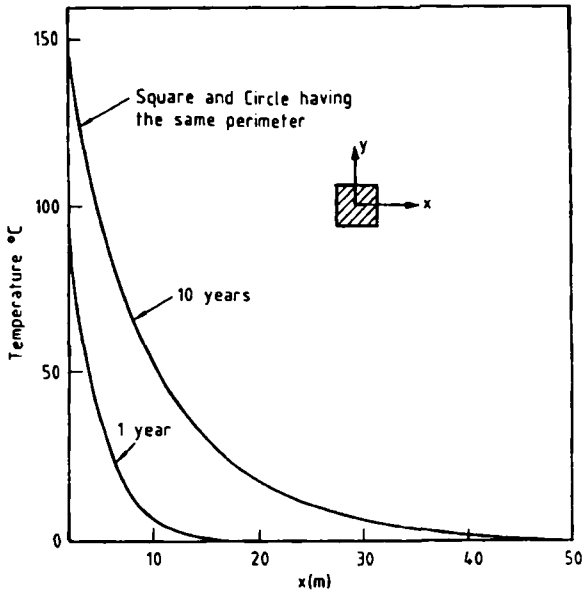

Figure 13. Comparison of the temperature distribution along the x-axis of a square heat source and a circular heat source of the same strength; square and circle are of equal cross-sectional perimeter

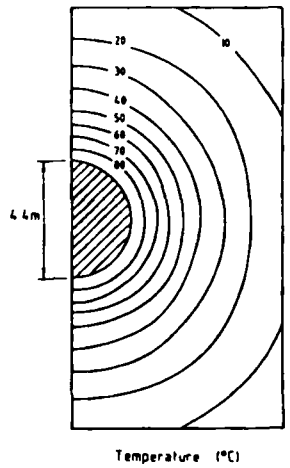

Figure 14. Contours of temperature surrounding a circular exponentially decaying heat source with equal cross-sectional perimeter to the square heat source shown in Figure 9, 1 yr after placement of the source

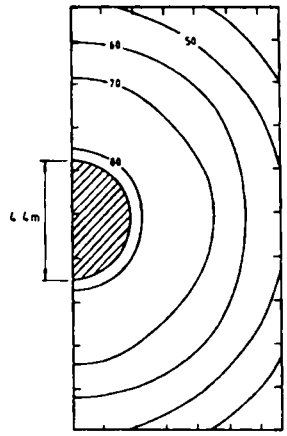

Figure 15. Contours of excess pore pressure surrounding a circular exponentially decaying heat source with equal cross-sectional perimeter to the square heat source shown in Figure 9, 1 yr after placement of the source

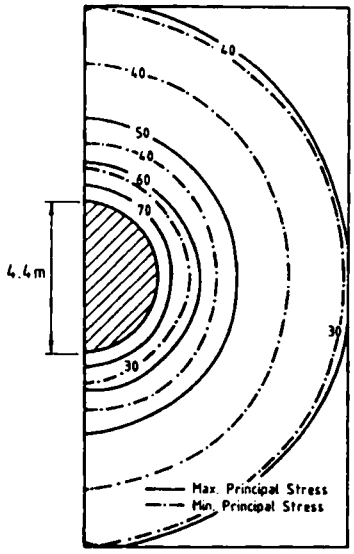

Figure 16. Contours of incremental maximum and minimum principal effective stress surrounding a circular exponentially decaying heat source of equal cross-sectional perimeter as the square heat source shown in Figure 11, 1 yr after placement of the source

pore pressure and the incremental principal stress contours are all very close to those for a square heat source, thereby demonstrating that the geometry of the heat source only has a significant influence on the field variable close to the heat source.

(c) *Effects of single heat generating waste 'canister' outside a square access tunnel*

An alternative repository design option is to locate the heat generating waste in a rectangular 'canister' to the side of a main access tunnel as shown in Figure 17. In this case, the traction free

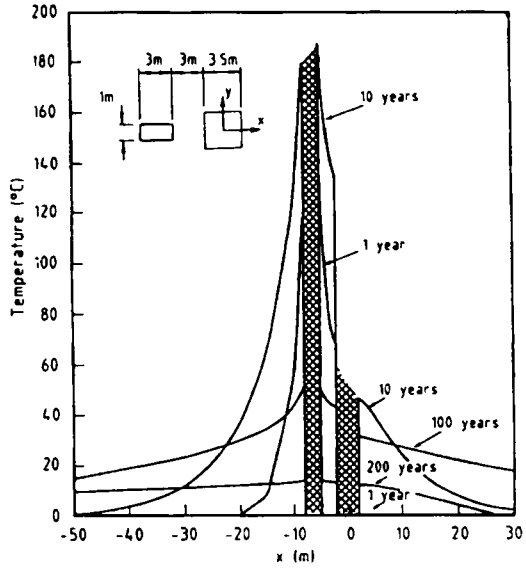

Figure 17. Temperature distribution at various times along the x-axis for a rectangular heat source with 'access' tunnel located to one side; note zero fluid and heat flux at the wall of the 'access' tunnel

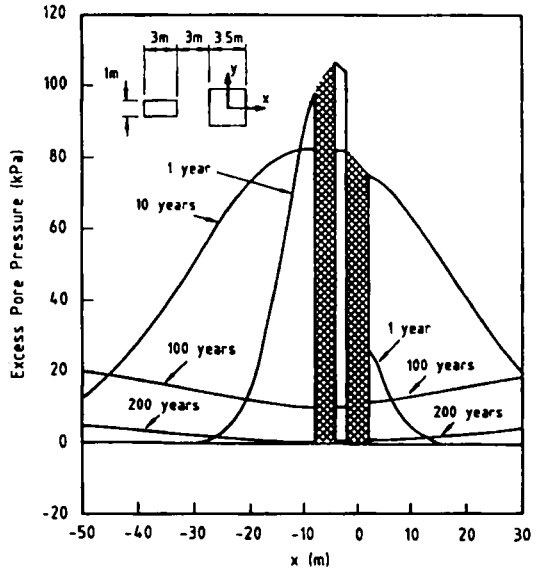

Figure 18. Excess pore pressure distribution at various times along the x-axis for a rectangular heat source with 'access' tunnel located to one side; note zero fluid and heat flux at the wall of the 'access' tunnel

access tunnel wall is assumed to have zero heat flux and fluid flow, while the canister is assumed to again provide an initial thermal loading of 1000 W m^{-1} run of repository and that the strength of the heat sources decays exponentially over time with a half-life of 30 yr.

In this case, the maximum temperature estimated after 10 yr shown in Figure 17, is slightly higher than the primary option (185°C compared to 150°C). This is primarily due to having the

same thermal loading being confined a smaller cross-sectional area ($3 \times 1\,m^2$ compared to a $3{\cdot}5 \times 3{\cdot}5\,m^2$). The excess pore pressures generated are also a little higher than for the primary option (Figure 18), but overall the temperature and excess pore water pressures are similar to the primary option.

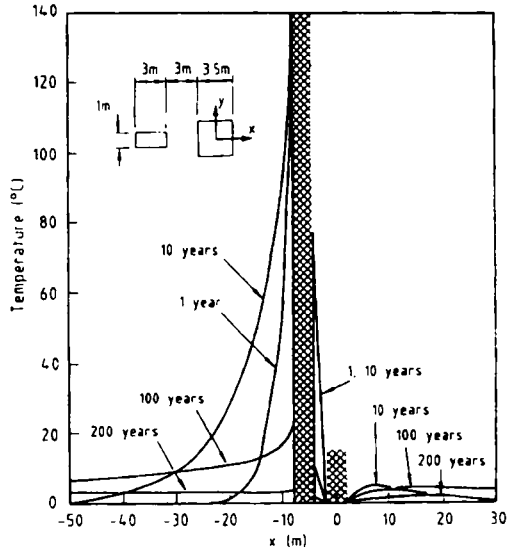

Figure 19. Temperature distribution at various times along the x-axis for a rectangular heat source with 'access' tunnel located to one side; note zero excess pore fluid pressure and temperature increment at the wall of the 'access' tunnel

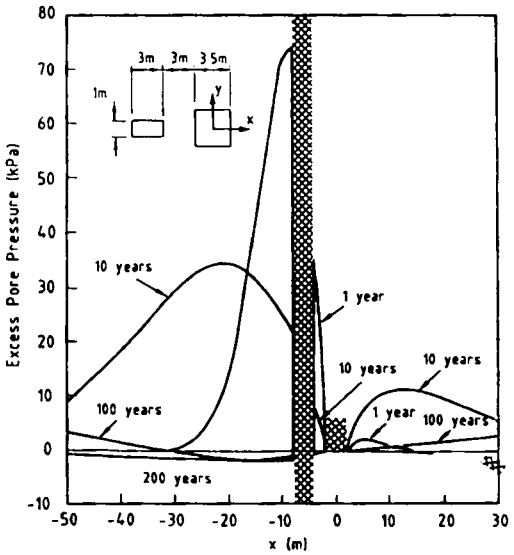

Figure 20. Excess pore pressure distribution at various times along the x-axis for a rectangular heat source with 'access' tunnel located to one side; note zero excess pore fluid pressure and temperature increment at the wall of the 'access' tunnel

It is interesting to again consider the same repository design and investigate the influence of a zero temperature and excess pore pressure change at the wall of the access tunnel. Practically, these conditions could be approximated by circulating a cooling fluid through the 'access' tunnel. For this case, the temperature and excess pore pressure along the x-axis of the global co-ordinate system are shown in Figures 19 and 20. It is observed that there is a distinct 'shadowing' effect provided by the access tunnel opposite to that of the heat source. Of course, this is due to the tunnel acting as a heat and fluid sink. In this case, it is found that the maximum temperatures at the canister wall are approximately the same as for the primary option (150°C), despite having the same thermal loading confined to a smaller cross-sectional area.

CONCLUSIONS

In the introduction to this paper, the circumstances under which a linear thermoelastic theory of consolidation induced to a heat source may be adopted as a suitable model to assist the design of secure radioactive waste repositories in a geologic host material has been discussed. It was concluded that provided a design approach based on technical conservatism is adopted, it is likely that a linear thermo-elastic consolidation theory could be a valuable design tool for the design of radioactive waste repositories. Based on this premise, the authors have carefully detailed the governing equations and boundary conditions for a thermo-poro-elastic solid and then developed a boundary element method for the numerical solution of these equations. The approach adopted is a Laplace transform boundary element method that had been previously demonstrated to be computationally efficient and accurate for the analysis of the equations governing uncoupled thermoelasticity, coupled thermoelasticity and poroelasticity.

The authors have presented a straightforward derivation of a boundary integral equation for fully coupled linear thermo-poro-elasticity by employing the properties of the Dirac delta function. A simple approximation of the exact boundary integral equations for a boundary element analysis is presented, and details of the numerical procedure provided. It was found that accurate thermal, excess pore pressure and displacements were obtained using relatively few boundary elements. The integral formulation, its boundary element approximation, and Green's functions required to implement the boundary element analysis, were all validated by comparison with a known analytic solution to the equations of fully coupled linear thermoelastic consolidation. From a computational viewpoint, an important finding is that the adoption of a Laplace transform boundary element method has enabled accurate solutions to be obtained while retaining the defining feature and appeal of the boundary element method for numerical analysis, namely, integrations over the bounding surface alone. This is contrasted with alternate time-stepping boundary element formulations that require the evaluation of domain integrals.

Using realistic material parameters for clay-like soils, it has been found that the temperature distribution for a cylinder with an axial heat source is essentially independent of the $c/\varkappa$ ratio, implying that there is little improvement to be had on the uncoupled theory for estimating the temperature distribution in a clay-like soil surrounding a heat source. By examining analytic and boundary element solutions for the axially heated cylinder, field variables that show a marked variation with the $c/\varkappa$ ratio have been identified and it is possible that numerical investigations such as those detailed here, may prove useful for the experimental determination of this important material property governing the behaviour of thermally consolidating materials.

The temperature, excess pore pressure and stress distribution induced by an exponentially decaying heat source buried deep underground has been investigated by means of several illustrative examples involving realistic material properties. This has demonstrated that the boundary element method developed here is capable of solving problems of practical interest.

Perhaps the most important finding from the viewpoint of the numerical analysis of the illustrative examples involving a thermo-poro-elastic materials, is that the Laplace transform boundary element method proved to be as robust, computationally efficient and as accurate as it has proven to be when analysing the equations of uncoupled thermo-elasticity, coupled thermoelasticity and poroelasticity.

From the viewpoint of the physical behaviour of the clay-like soil, the most important findings are that the uncoupled theory of heat transfer is adequate for the prediction of temperature increments within the soil mass, but that there is strong coupling between the excess pore fluid pressure and the displacement and temperature fields, and that these couplings should not be neglected. From a repository design viewpoint, an important finding is that thermal design requirements are likely to offer significant constraints on the repository design. The high temperatures close to the radioactive heat source noted at early times reinforces the view that temporary above-ground storage offers the potential for significantly lowering soil temperatures in the immediate vicinity of the heat source.

For the illustrative examples considered here, it is found that while the shape of the heat source has a pronounced effect on the field variables close to the source, the influence of repository shape is negligible a short distance from the repository. For this reason, it is expected that further investigations will show that, provided temperatures are not excessive, the shape of the repository containing the heat generating material has little influence on the long term performance of the soil to act as a barrier preventing the dispersion of radionuclids to the biological environement.

APPENDIX I

In this appendix we detail a physical interpretation of the constants found in the equations governing linear thermoelastic consolidation of a granular material. This is done in quite a straightforward way, and is based on several conceptually simple tests.

To begin, it is apparent that if the temperature and pore fluid pressure are held constant, the usual linear elastic stress–strain relations are obtained from equation (2). Hence it follows that the constants G and λ are the familiar Lame constants under isothermal, drained conditions. Now for isothermal conditions (i.e. $\theta = 0$), it is expected that the well known Biot theory of consolidation should be recovered from equations (2) and (4) (Biot, 1941). To obtain this result we require that $\chi_0 = \chi_1$. Further, for isobaric conditions (i.e. $p = 0$), it would be expected that the well known fully coupled thermoelastic theory would be recovered from equations (2) and (5).[60] To obtain this result we require that $\beta_0 = \beta_1$.

Having established these relationships, a physical interpretation of the constants in equations (2)–(5) can be obtained by considering two conceptually simple tests. For this purpose, it will only be necessary to consider Hooke's law in the form,

$$\frac{\sigma_{kk}}{3} = \frac{e_v}{C} - \chi_0 p - \beta_0 \theta, \tag{34}$$

where C is the incremental compressibility of soil skeleton under isothermal drained conditions (i.e. $C = 3(1 - 2\nu)/E$), E is the Young's modulus of the soil under isothermal drained conditions and ν is the Poisson's ratio under drained isothermal conditions.

Suppose that a sample of saturated porous material is first subjected to an all round pore fluid pressure increment (p_0) under isothermal undrained conditions so that the excess pore fluid pressure increases to p_0 and the stress state of the element is hydrostatic. It seems reasonable to assume that under such conditions the stress state of the skeleton will also be hydrostatic and so it is possible to calculate the skeletal strain and so the strain of the sample. Similarly, it seems

reasonable that the change in entropy of the sample tested will be the sum of the entropy changes of its component parts.

The second physical test to be considered is conducted on a sample of material subjected to a uniform increase in temperature θ_0 under conditions of constant total stress and excess pore fluid pressure. Again it seems reasonable to assume that both soil skeleton and skeletal material will undergo uniform thermal strain and that the increase in entropy of the sample will be the sum of the increase in entropy of its component parts. For these two tests, the field quantities take the values shown in Table II.

Now defining the quantities in Table II, C_s is the compressibility of the *skeletal material* under isothermal conditions (compare with earlier definition of C), (i.e. $C_s = 3(1 - 2\nu_s)/E_s$), E_s is the Young's modulus of the skeletal material under isothermal drained conditions, ν_s is the Poisson's ratio of the skeletal material under drained isothermal conditions, C_f is the compressibility of the pore fluid under isothermal conditions, a_s is the linear coefficient of thermal expansion of the soil skeleton, a_f is the linear coefficient of thermal expansion of the pore fluid, ϱ_s is the density of the skeletal material, ϱ_f is the density of the pore fluid, c_{ps} is the specific heat of the skeletal material at constant pressure, c_{pf} is the specific heat of the pore fluid at constant pressure, n_0 is the initial porosity, S is the increment in entropy within the reference element, ς is the increment of fluid volume within the reference element and T_0 is the absolute temperature.

While most of the entries shown in Table II are easily deduced from well known physical behaviours of materials, the entries in Table II for the change in entropy are perhaps less well known. However, the entry for the entropy change associated with isobaric non-isothermal test is easily deduced directly from the definition of the change in entropy of reference element, viz,

$$S = \frac{\Delta q}{T_0} \tag{35}$$

where Δq is the increment in thermal energy within the reference element.

The entry for the change in entropy associated with the isothermal pressure test is, though, less easily found. However, the quantity shown in Table II can be deduced in the following way. It is clear from the theory of fully coupled thermoelasticity that an increase in pressure leads to an increase in temperature of the material. For an isothermal pressure test described, viz., $\theta = 0$, this implies heat must leave the reference volume. As heat and so entropy is lost from the reference volume, this accounts for the minus sign associated with the entry. Now, provided the isothermal pressure test is performed sufficiently slowly so that 'reversible' thermodynamic conditions are approximated, the fully coupled theory of thermoelasticity indicates that the change in entropy of the material in the reference element undergoing the isothermal pressure test is given by,[31,65]

$$S = (1 - n_0)\beta_s e_{vs} + n_0 \beta_f e_{vf} \tag{36}$$

Table II. Expected material response

Field quantity	Isothermal pressure increase	Isobaric temperature increase
p	p_0	0
θ	0	θ_0
$\sigma_{kk}/3$	$-p_0$	0
e_v	$-p_0 C_s$	$3a_s\theta_0$
ς	$n_0(C_f - C_s)p_0$	0
S	$-3((1 - n_0)a_s + n_0 a_f)p_0$	$\left((1 - n_0)\frac{\varkappa_s c_{ps}}{T_0} + n_0 \frac{\varkappa_f c_{pf}}{T_0}\right)\theta_0$

where β_s and β_f are the thermal moduli of the skeletal material and the pore fluid respectively, while e_{vs} is the volumetric strain of the skeletal material and e_{vf} is the volumetric strain of the pore fluid. Now noting the following relations,

$$e_{vs} = -p_0 C_s; \quad e_{vf} = -p_0 C_f; \quad \beta_s = 3a_s/C_s; \quad \beta_f = 3a_f/C_f \tag{37}$$

and substituting these values into equation (36) leads directly to the entry in Table II.

Having established the origin of the entries shown in Table II, the values for the isothermal pressure test may now be substituted directly into equations (4), (5) and (34) revealing the following relations,

$$-p_0 = -\frac{C_s}{C} p_0 - \chi_0 p_0, \qquad n_0(C_f - C_s)p_0 = -\chi_0 C_s p_0 + J p_0$$

$$-3((1-n_0)a_s + n_0 a_f)p_0 = -\beta_0 C_s p_0 - Y_1 p_0 \tag{38}$$

while substitution of the entries in Table II for the isobaric temperature test leading to the following relations,

$$0 = \left(1 - \frac{C_s}{C}\right), \qquad -3n_0(a_f - a_s)\theta_0 = 3\chi a_s \theta_0 + Y_0 \theta_0,$$

$$\left((1-n_0)\frac{\varrho_s c_{ps}}{T_0} + n_0 \frac{\varrho_f c_{pf}}{T_0}\right)\theta_0 = 3\beta a_s \theta_0 + Z\theta_0. \tag{39}$$

By simple algebraic rearrangement, it is therefore found that the material constants in the linear theory of thermoelastic consolidation have the following physical interpretations, viz,

$$\chi_0 = \left(1 - \frac{C_s}{C}\right), \qquad \beta_0 = \frac{3a_s}{C}, \qquad J = n_0(C_f - C_s) + \chi_0 C_s$$

$$Y_1 = -3n_0(a_f - a_s) - 3a_s\left(1 - \frac{\beta C_s}{3a_s}\right) = Y_0 = -3n_0(a_f - a_s) - 3\chi_0 a_s$$

$$Z = \left((1-n_0)\frac{\varrho_s c_{ps}}{T_0} + n_0 \frac{\varrho_s c_{ps}}{T_0}\right) - \beta^2 C \tag{40}$$

We note here that equivalent expressions for χ_0 and J were obtained by Biot and Willis[66] for Biot's theory of isothermal consolidation.

Now past experience has shown that most if not all material properties for any real material are likely to be functions of the excess pore fluid pressure and the ambient temperature. For example, it is well known that the coefficient of linear expansion and density are temperature dependent properties, however, in the linear theory presented here, these effects have been neglected. In addition, geometric non-linearities present in the specified tests have been neglected on the assumption that they represent second order effects. For example, the change in porosity accompanying an isothermal pressure increase and the convected entropy transported into the reference element due to the change in mass of pore fluid within the reference element are not considered in the linear theory presented here. For these reasons, it is unlikely that the relations shown in Table II will hold for any real material. However, we note that this discrepancy between real and idealised material behaviour can be minimized by estimating the material parameters of the linear thermoelastic consolidation theory under experimental test conditions as close as possible to field conditions, and restricting the magnitude of imposed changes.

Finally, we mention that a more rigorous approach for deducing the symmetry of the material constants appearing in the equations of linear thermoelastic consolidation may be found by means of an explicit assumption as to the existence of a conservative internal energy function for the material. This assumption was only implied in the 'intuitive' requirement that the equations of

linear thermoelastic consolidation reduce to Biot's theory under isothermal conditions, and reduce to the equations of fully coupled thermoelasticity under isobaric conditions. However, by means of an explicit assumption as to the existence of an internal energy function, the symmetry of the governing equations may be deduced using the theory of calculus of exact differentials. This approach has been adopted by numerous previous authors (eg. Biot,[64] Nowacki,[31] Cleary,[34] McTigue,[26]). However, we note that a physical interpretation of the material constants cannot be deduced from thermodynamic considerations alone.

REFERENCES

1. Uranium Institute, 1991.
2. R. A. Forsch, 'Disposing of high-level radioactive waste', *Oceanus*, **20**(1), 5–17 (1977).
3. T. A. Littlefield and N. Thornley, *Atomic and Nuclear Physics*, Van Nostrand, London, 1963.
4. A. J. Silva, 'Physical processes in deep-sea clays', *Oceanus*, **20**, 31–40 (1977).
5. G. R. Heath, 'Barriers to radioactive waste migration', *Oceanus*, **20**, 26–30 (1977).
6. (NEA), Nuclear Energy Agency 'Siting of Radioactive Waste Repositories in Geological Formations', *Workshop Proc.*, OECD, 1981.
7. C. D. Hollister, 'The sealed option', *Oceanus*, **20**(1), 18–25 (1977).
8. C. D. Hollister, D. R. Anderson and G. R. Heath, 'Seabed disposal of nuclear wastes', *Science*, **213**(4514), 1321–1326 (1981).
9. R. M. Quigley and R. K. Rowe, 'Leachate migration through clay below a domestic waste landfill, Sarnia, Ontario, Canada'; Chemical interpretactive and modelling philosophies', *Hazardous and Industrial Solid Waste Testing and Disposes; Sixth Volume*, ASTM STP 933, (1986).
10. D. D. Desaulniers, J. A. Cherry and P. Fritz, 'Origin, age and movement of pore water in argillaceous quaternary deposits at four sites in South-Western Ontario', *J. Hydrol.* **50**, 231–257 (1981).
11. R. K. Rowe and D. W. Sawicki, 'The modelling of a natural diffusion profile and the implications for landfill design', in Pande and Pietruszczak (eds.) *Numerical Methods in Geomechanics*, Balkema, Rotterdam, (1992) pp. 481–490.
12. R. A. Freeze and J. A. Cherry, Groundwater, Prentice-Hall, Eaglewood Cliffs, NJ, 1979.
13. C. W. Jeong and K. J. Lee, 'Propagation of concentration waves through a sorption medium with similtaneous ion exchange and electrolyte adsorption', *Waste Management*, **12**, 61–73 (1992).
14. I. R. De Bruyn, Nuclear Resarch Centre, Geologic Waste Disposal Project, Boeretang, Brussels, 1992, private communication.
15. P. J. Hensley and C. Savvidou, 'Modelling coupled heat and contaminant transport in groundwater', *Int. J. numer. anal. methods geomech.: Geo-environmental Issue*, **17**, 483–527 (1993).
16. C. E. Hickox and H. A. Watts, 'Steady thermal convection from a concentrated source in a porous medium', *Trans. ASME*, **102**, 248–253 (1980).
17. C. Savvidou, Effect of a heat source in saturated clay, *Ph.D. Thesis*, Cambridge University, 1984.
18. T. Hueckel and A. Peano, 'Some geotechnical aspects of radioactive waste isolation in continental clays', *Comput. Geotech.* **3**, 157–182 (1987).
19. A. M. Britto, C. Savvidou, D. V. Maddocks, M. J. Gunn and J. R. Booker, 'Numerical and centrifuge modelling of coupled heat flow and consolidation around hot cylinders buried in a clay', *geotechnique*, **39**(1), 13–25 (1989).
20. R. W. Lewis, C. E. Majorana and B. A. Schrefler, 'A coupled finite element model for consolidation of a non-isothermal elastoplastic media', *Transport in Porous Media*, **1**, 155–178 (1986).
21. R. W. Lewis, P. J. Roberts and B. A. Schrefler,, 'Finite element modelling of two phase heat and fluid flow in deforming porous media', *Transport in Porous Media*, **14**, 319–344 (1989).
22. J. R. Booker and C. Savvidou, 'Consolidation around a spherical heat source', *Int. J. Solids Struct.* **20**, 1079–1090 (1984).
23. J. R. Booker and C. Savvidou, 'Consolidation around a point heat source', *Int. J. numer. anal. methods geomech.*, **9**, 173–184 (1985).
24. Savvidou and Booker, 1988.
25. C. Savvidou and J. R. Booker, 'Consolidation around a heat source buried deep in a porous thermoelastic medium with aisotropic flow properties', Int. J. numer. anal. methods geomech. **13**, 75–90 (1989).
26. D. F. McTigue, 'Thermoelastic response of a fluid saturated porous rock', *J. Geophys. Res.* **91**(B9), 9533–9542 (1986).
27. M. D. Greenburg, *Applications of Green's Functions in Science and Engineering*, Prentice-Hall, Englewood Cliffs, New Jersey, 1971.
28. D. W. Smith and J. R. Booker, 'Boundary integral analysis of transient thermoelasticity', *Finite Elements in Engineering, Proc. 5th Int. Conf. in Australia on Finite Element Methods*, University of Melbourne, in: J. F. Williams and L. K. Stevens, (eds.), University of Melbourne, Melbourne, 1987.
29. D. W. Smith and J. R. Booker, 'Boundary integral analysis of transient thermoelasticity', int. J. numer. anal. methods geomech., **13**, 283–302 (1989).
30. D. W. Smith and J. R. Booker, 'Numerical analysis of linear quasi-static coupled transient thermoelasticitiy', in: G. Swoboda, (ed.), *Numerical Methods in Geomechanics*, Innsbruck, A. A. Balkema, Rotterdam, 1988.

31. W. Nowacki, *Thermoelasticity*, Pergamon Press, Oxford, 1962.
32. V. Sladek and J. Sladek, 'Boundary integral equation method in thermoelasticity, part I: general analysis', *Appl. Math. Modelling*, **7**, 241–253 (1983).
33. M. A. Biot, 'General solutions of the equations of elasticity and consolidation for a porous material', *J. App. Mech.* **23**(1), 91–96 (1956).
34. M. P. Cleary, 'Fundamental solutions for a fluid saturated porous solid', *Int. J. Solids Struct.* **13**, 785–806 (1977).
35. A. H. D. Cheng and J. A. Ligget, 'Boundary integral equation method for linear porous-elasticity with application to soil Consolidation', *Int. J. Numer. Meth. Eng.*, **20**, 279–296 (1984).
36. A. H. D. Cheng and E. Detournay, 'A direct boundary element method for plane strain poroelasticity', *Int. J. Numer. Anal. Meth. Geomech.* **12**, 551–572 (1988).
37. J. R. Booker and D. W. Smith, 'Behaviour of a heat source in a fully coupled saturated thermoelastic soil', in: S. Pietruszczak and G. N. Pande, (eds.) *Numerical Methods in Geomechanics*, NUMOG III, Elsevier Applied Science, London, 1989, pp. 399–406.
38. D. W. Smith, 'Boundary element analysis of heat flow and consolidation for geotechnical applications', *Ph.D. Thesis*, University of Sydney, Sydney, 1990.
39. D. W. Smith and J. R. Booker, 'Green's functions for a fully coupled thermo-poro-elastic material', *Int. J. numer. anal. methods geomech.*, **17**, 139–163 (1993).
40. R. L. Schiffman, 'A thermoelastic theory of consolidation', *Environ. Geophys. Heat Transfer*, **4**, 78–84 (1972).
41. W. Derski and S. J. Kowalski, 'Equations of linear consolidation', *Arch. Mech.* **31**, 303–316 (1979).
42. Palcianskar and Domenico, 1982.
43. J. Noorishad, C. F. Tsang and P. A. Witherspoon, 'Coupled thermal–hydraulic–mechanical phenomena in saturated in porous rocks: numerical approach, *J. Geophys. Res.* **89**(B12), 10365–10373 (1984).
44. B. L. Aboustit, S. H. Advani and J. K. Lee, 'Variational principles and finite element simulations for thermo-elastic consolidation', *Int. J. numer. methods geomech.*, **9**, 49–69. (1985).
45. C. C. Mei and P. A. Tyvand, 'Thermal consolidation of a thick and soft soil layer', *ASCE J. Eng. Mech.* **114**(6), 990–1009 (1988).
46. D. Nardina and C. A. Brebbia, 'The solution of parabolic and hyperbolic problems using an alternative boundary element formulation', in: C. A. Breebbia (ed.), *Boundary Elements* VII, Springer, Berlin, 1985.
47. P. K. Banerjee, R. Bulterfield and G. R. Tomlin, 'Boundary element methods for two-dimensional problems of transiant groundwater flow, *Int. J. numer. anal. methods. geomech*, **5** 15–31, (1981).
48. V. Rources and E. Alarcon, 'Transient heat conduction problems using the B.I.E.M.', *Comp. Struct.*, **16**, 717–730 (1983).
49. M. Tanaka, H. Togoh and M. Kikuta, 'An application of the boundary element method to thermoelastic problems', *Fifth Internationl Conference on Boundary Elements*, Ed. Brebbia *et al.*, 417–426 (1983).
50. S. Sharp and S. L. Crouch, 'Boundary integral methods for thermoelastic problems', *J. Appl. Mech.* **53**, 298–302 (1986).
51. A. Taigbenu and J. A. Ligget, 'An integral formulation applied to diffusion and Boussinesq equations', *Int. J. Numer. Meth. Eng.*, **23**, 1057–1079 (1986).
52. A. Chaudouet, 'Three dimensional transient thermo-elastic analysis by the BIE method', *Int. J. numer. methods engg.* **24**, 24–45 (1989).
53. D. Henry and P. K. Banarjee, 'A new boundary element formulation for two and three dimensional thermoelasticity using particular integrals', *Int. J. Numer. Meth. Eng.*, **26**, 2061–2077 (1988).
54. Saigal et al., 1990.
55. A. Talbot, 'The accurate numerical inversion of Laplace transforms', *J. Inst. Math. Appl.* **23**, 97–120 (1979).
56. F. J. Rizzo and D. J. Shippy, 'A method of solution for certain problems of transient heat conduction', *AIAA J.*, **8**(11), 2004–2009 (1970).
57. V. Sladek and J. Sladek, 'Boundary integral equation method in thermoelasticity, part III: uncoupled thermoelasticity', *Appl. Math. Modelling*, **8**, 413–418 (1984).
58. D. W. Smith, J. P. Carter and J. R. Booker, 'Numerical analysis of linear quasi-static coupled transient thermoelasticity', *Computational Techniques and Applications: CTAC 87*, Proc. of the 1987 International Conference, University of Sydney, Ed. Noye, J. and Fletcher, C., Pub. North-Holland, Amsterdam, (1987).
59. A. H-D. Cheng and E. Detournay, 'A direct boundary element method for plane strain poroelasticity', *Int. J. numer. anal. methods geomech.* **12**, 551–572 (1988).
60. B. A. Boley ad J. H. Weiner, *Theory of Thermal Stresses*, Wiley, New York, 1960.
61. M. J. Lighthill, *Introduction to Fourier Analysis and Generalised Functions*, The Syndics of the Cambridge University Press, London, 1958.
62. S. L. Crouch and A. M. Starfield, '*Boundary element methods in solid mechanics*', George Allen and Unwin Ltd, London, (1983).
63. M. Abramowitz and I. Stegun, *Handbook of Mathematical Functions*, National Bureau of Standard Applied Mathematics, Ser. 55, US Government Printing Offices, Washington D.C., 1964.
64. M. A. Biot, 'General theory of three dimensional consolidation', *J. Appl. Phys.* **12**, 155–164 (1941).
65. R. O. Kestin, *A Course in Thermodynamics*, **Vols I and II**, (1965, 1968) Blaisdell, New York. A. Larsson, 'State-of-the-art report on radioactive waste disposal', *IAEA Bulletin*, No. 4/1989, pp. 18–25 (1989).
66. M. A. Biot and D. G. Willis, 'The elastic coefficients of the theory of consolidation', J. App. Mech. **24**(4), 594–601 (1957).
67. J. P. Carter and J. R. Booker, 'Elastic consolidation around a deep circular tunnel', *Int. J. Solids Struct.* **18**, 1059–1074 (1982).